Born-Kuhn model for magnetochiral effects

Hiroyuki Kurosawa* and Shin-ichiro Inoue
Advanced ICT Research Institute, National Institute of Information and Communications Technology (NICT), Kobe, Hyogo 651-2492, Japan

(Received 8 August 2018; published 5 November 2018)

This study focuses on theoretical and numerical investigations of the magnetochiral (MCh) effect in the optical region. Electrodynamics in a medium with broken time and space inversions is described by two orthogonal coupled oscillators, in what is known as the Born-Kuhn model, subject to an external static magnetic field. Constitutive equations and the refractive index of the medium are theoretically derived. The results show that the MCh effect is induced even in the absence of an intrinsic interaction between the magneto-optical effect and the optical activity. The study also numerically investigates the electromagnetic response in a metamaterial with magnetism and chirality in the deep ultraviolet region. The results agree well with the main results of our theory. This paper paves the way to realizing MCh metamaterials in the optical region.

DOI: 10.1103/PhysRevA.98.053805

I. INTRODUCTION

Symmetry is a key feature in physics. Among various kinds of symmetries, space and time inversion symmetries are important for controlling the polarization state of light. Breaking of space inversion symmetry gives rise to reciprocal polarization rotation known as optical activity (OA), which originates from electromagnetic induction in a chiral structure. Breaking of time inversion symmetry gives rise to nonreciprocal polarization rotation known as Faraday rotation. Faraday rotation is a magneto-optical (MO) effect, which originates from the Lorentz force on electrons in a material. Both the OA and the MO effects give rise to similar phenomena such as polarization rotation, but the physical origins of these phenomena are different. Therefore, interaction between the OA and the MO effects is expected to be not just a superposition but a product of those phenomena, resulting in a different effect. In a system with simultaneous breaking of space and time inversion symmetries, the absorption coefficient of a material irradiated with unpolarized light depends on the propagation direction of the light: directional birefringence is induced in the system. This effect is known as the magnetochiral (MCh) effect [1–4]. Owing to directional birefringence of unpolarized light, this effect is applicable to optical isolators. In particular, it may allow one-way mirrors to be realized. The MCh effect is also important in fundamental physics because it is key to realizing an artificial gauge field for light [5,6]. The MCh effect has been investigated in natural materials such as $CuFe_{1-x}Ga_xO_2$ [7] and CuB_2O_4 [8] exposed to a low temperature or a high external magnetic field.

As well as studies in natural materials, artificial structures have received considerable attention as a platform to investigate MCh effects. In the microwave region, a metamolecule composed of a twisted Cu wire and a ferrite rod placed within a waveguide exhibited a significantly enhanced MCh effect, two orders of magnitude greater than in previous studies [9–11]. The MCh effect is enhanced under preferable conditions for practical applications, namely, in a low magnetic field at room temperature. In the optical region, artificially controlled magnetochiral dichroism (MChD) has been reported in a Ni helix array under low external static magnetic fields at room temperature [12]. The helix array has both magnetism and structural chirality and gives rise to MChD. In addition, the combination of independent magnetic and chiral elements gives rise to MChD [13,14]. To understand MChD further, a theoretical model describing the independent control of magnetism and chirality is needed.

In this paper, we numerically demonstrate that an MCh effect is realized in the optical region by independent control of magnetism and structural chirality. We theoretically formulate the MCh effect based on a coupled Lorentz oscillator model in an external static magnetic field [15]. Our theoretical results indicate that the MCh effect is realized even in the absence of internal coupling between magnetism and chirality. Calculation predicts that a gigantic MCh effect can be realized in a metamaterial with simultaneous breaking of space and time inversion.

II. THE BORN-KUHN MODEL IN A STATIC MAGNETIC FIELD

We consider the situation shown in Fig. 1, where two identical oscillators separated by a distance d are coupled and subjected to an external static magnetic field. To describe the electrodynamics of this system, we start with the Born-Kuhn model [16], described as

$$\ddot{u}_x + \gamma \dot{u}_x + \omega_0^2 u_x + \omega_{\mathrm{Ch}}^2 u_y = \frac{q}{m^*}(e_x + i\omega u_y B_0), \quad (1)$$

$$\ddot{u}_y + \gamma \dot{u}_y + \omega_0^2 u_y + \omega_{\mathrm{Ch}}^2 u_x = \frac{q}{m^*}(e_y - i\omega u_x B_0), \quad (2)$$

where m^* is the effective mass, q is the electric charge, γ is the damping factor, and ω_0 is the resonance frequency of the oscillator. The imaginary unit is denoted i. The x and y components of the electric field on the oscillator are described

*kurosawa.hiroyuki@nict.go.jp

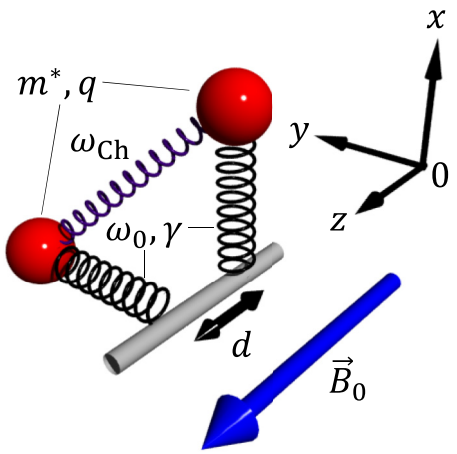

FIG. 1. Schematic of two coupled oscillators separated by distance d and with resonance frequency ω_0 and damping constant γ. An external magnetic field is applied along the $+z$ direction.

by e_x and e_y, respectively. The coupling constant between the two oscillators is given by $\omega_{\rm Ch}$. The displacement of the oscillator is $\vec{u} = (u_x, u_y)$. An overdot denotes a derivative with respect to time. We solve the equations of motion for coupled oscillators under an external magnetic field B_0 directed in the $+z$ direction.

We expand the position vector of the oscillators to be $\vec{u} = \vec{u}^{(0)} + \vec{u}^{(1)}$, where the superscripts (0) and (1) denote the zeroth- and first-order spatial dispersion. At zeroth order, the coupling effect between the two oscillators is negligible, resulting in $\omega_{\rm Ch} = 0$. The zeroth-order coupled equation gives us the solution as

$$\begin{pmatrix} u_x^{(0)} \\ u_y^{(0)} \end{pmatrix} \simeq \frac{q}{m^*\Omega^2} \begin{pmatrix} 1 & i\omega\Omega_{\rm c}/\Omega^2 \\ -i\omega\Omega_{\rm c}/\Omega^2 & 1 \end{pmatrix} \begin{pmatrix} e_x \\ e_y \end{pmatrix}, \quad (3)$$

where $\Omega = \sqrt{\omega_0^2 - \omega^2 - i\gamma\omega}$ and the cyclotron frequency $\Omega_{\rm c} = qB_0/m^*$. The off-diagonal component of the square matrix represents the MO effect, giving rise to Faraday rotation.

At first order, the equation of motion is described as

$$\ddot{u}_x^{(1)} + \gamma\dot{u}_x^{(1)} + \omega_0^2 u_x^{(1)} + \omega_{\rm Ch}^2 u_y^{(0)} = 0, \quad (4)$$

$$\ddot{u}_y^{(1)} + \gamma\dot{u}_y^{(1)} + \omega_0^2 u_y^{(1)} + \omega_{\rm Ch}^2 u_x^{(0)} = 0. \quad (5)$$

In this coupled equation, we dropped the electric Lorentz force of first order, which is calculated to be $\vec{e}(\vec{u}^{(0)} + \vec{u}^{(1)})|_{1\rm st} \simeq (\vec{u}^{(1)} \cdot \nabla)\vec{e}(\vec{u}^{(0)}) = -i(\vec{u}^{(1)} \cdot \vec{k})\vec{e}$. This is 0 because the displacement vector is perpendicular to the wave vector. The first-order coupled equation gives us the solution as

$$\begin{pmatrix} u_x^{(1)} \\ u_y^{(1)} \end{pmatrix} = -\left(\frac{\omega_{\rm Ch}}{\Omega}\right)^2 \frac{qd}{m^*\Omega^2} \begin{pmatrix} 0 & -ik \\ ik & 0 \end{pmatrix} \begin{pmatrix} e_x \\ e_y \end{pmatrix} - \left(\frac{\omega_{\rm Ch}}{\Omega}\right)^2 \frac{q}{m^*\Omega^2} \frac{dk\omega\Omega_{\rm c}}{2\Omega^2} \begin{pmatrix} e_x \\ e_y \end{pmatrix}. \quad (6)$$

The first term on the right-hand side of Eq. (6) represents the OA. The second term is proportional to the cyclotron frequency $\Omega_{\rm c}$ characterizing the magnetism and to $\omega_{\rm Ch}$ characterizing the chirality. This term is proportional to the wave vector k, representing the directional birefringence. That is, the second term represents the MCh effects.

So far, we have solved the coupled oscillators up to the first order of spatial dispersion and obtained the displacement vector $\vec{u} = \vec{u}^{(0)} + \vec{u}^{(1)}$. From this result, we can calculate a polarization vector $\vec{p} = q\vec{u}$. Here, we convert the microscopic polarization and electric field to macroscopic quantities by taking a volume average; that is, $\vec{P} = N\langle\vec{p}\rangle$ and $\vec{E} = \langle\vec{e}\rangle$, where N is the density of the oscillator and $\langle\ \rangle$ indicates the volume average. Using Maxwell's equation $\nabla \times \vec{E} = i\omega\vec{B}$, we obtain constitutive equations for the electric displacement $\vec{D}$ and the magnetic-field strength $\vec{H}$ as

$$\vec{D} = \varepsilon_0\hat{\varepsilon}\vec{E} - i\xi\sqrt{\frac{\varepsilon_0}{\mu_0}}\vec{B} - 2\varepsilon_0\frac{\xi g}{\varepsilon - 1}\frac{ck}{\omega}\vec{E}, \quad (7)$$

$$\vec{H} = \mu_0^{-1}\vec{B} - i\xi\sqrt{\frac{\varepsilon_0}{\mu_0}}\vec{E}, \quad (8)$$

where ε_0 is the permittivity and μ_0 is the permeability of the vacuum. In these constitutive equations, we introduce notations defined as

$$\hat{\varepsilon} = \begin{pmatrix} \varepsilon & ig \\ -ig & \varepsilon \end{pmatrix}, \quad (9)$$

$$\varepsilon = 1 + \frac{2}{3}\frac{\omega_p^2}{\omega_0^2 - \omega^2 - i\gamma\omega}, \quad (10)$$

$$g = \frac{2}{3}\frac{\omega_p^2}{\omega_0^2 - \omega^2 - i\gamma\omega}\frac{\omega\Omega_{\rm c}}{\omega_0^2 - \omega^2 - i\gamma\omega}, \quad (11)$$

$$\xi = \frac{1}{3}\frac{\omega_p^2}{\omega_0^2 - \omega^2 - i\gamma\omega}\frac{\omega_{\rm Ch}^2}{\omega_0^2 - \omega^2 - i\gamma\omega}\frac{d}{2}\frac{\omega}{c}, \quad (12)$$

where ω_p is the plasma frequency, defined as $\sqrt{Nq^2/(\varepsilon_0 m^*)}$. Note that the factor $2/3$ in ε and g stems from the volume average and is the consequence of the two orthogonal oscillators along the x and y directions in three-dimensional space. The remaining direction is related to the OA, resulting in the factor $1/3$ in ξ. The constitutive equations are linked to the Born-Kuhn model under the external magnetic field as follows. Due to the applied external dc magnetic field, the MO effect appears in the of-diagonal components of the permittivity, which is described in Eqs. (9) and (11). The orthogonal oscillators give rise to the OA, which appears as ξ in Eqs. (7) and (8). As a result of coupling between these two effects, the MCh effect appears in the last term on the right-hand side of Eq. (7).

Following the derivation of the constitutive equations, let us consider wave propagation in an MCh medium. Substituting the constitutive equations into Maxwell's equations, we obtain the wave equation

$$\nabla^2\vec{E} + \left(\frac{\omega}{c}\right)^2(\varepsilon\vec{E} + i\vec{E} \times \vec{g}) - 2\xi\frac{\omega}{c}\nabla \times \vec{E} - 2\frac{\omega}{c}\frac{\xi g k}{\varepsilon - 1}\vec{E} = 0, \quad (13)$$

where we assume that the electromagnetic wave is transverse: $\nabla \cdot \vec{E} = 0$. Assuming that the eigenstate of this system is

circular polarization, we obtain the eigenequation

$$(\varepsilon \mp g)\left(\frac{\omega}{c}\right)^2 \mp 2\xi k\left(1 \pm \frac{g}{\varepsilon - 1}\right)\frac{\omega}{c} - k^2 = 0, \quad (14)$$

where $\mp$ corresponds to right and left circular polarizations, respectively. The solution of this quadratic equation with respect to ω/c yields the dispersion relation:

$$\frac{\omega}{c} = \frac{|k|}{\sqrt{\varepsilon \mp g} \mp \xi \mathrm{sgn}(k) - \xi \mathrm{sgn}(k) g/(\varepsilon - 1)}. \quad (15)$$

The denominator on the right-hand side of Eq. (15) is a refractive index, which is approximated to be

$$n = \sqrt{\varepsilon} \mp \frac{g}{2\sqrt{\varepsilon}} \mp \xi \mathrm{sgn}(k) - \xi \mathrm{sgn}(k)\frac{g}{\varepsilon - 1}. \quad (16)$$

This refractive index consists of four terms. The first term is the conventional refractive index, which is independent of the polarization state and propagation direction of the light. The second term represents the MO effect, which is dependent on the polarization state. The third term corresponds to the OA, which is dependent on both the polarization state and the propagation direction. The last term includes the product of ξ and $g/(\varepsilon - 1)$. This term is dependent on the propagation direction but is independent of the polarization state, representing the MCh effect. In our derivation of the MCh effect, the MO effect is formulated at zeroth order and is modulated by the OA at first order, resulting in the MCh effect. This cascade process is found in the second term on the left-hand side of Eq. (14). This term is proportional to $\mp\xi$ and represents the OA. Moreover, it has a correction term described as $\pm g/(\varepsilon - 1)$, which represents the MO effect. The product of $\mp\xi$ and $\pm g/(\varepsilon - 1)$ describes the modulation of the MO effect by the OA and gives $-\xi g/(\varepsilon - 1)$, which appears in the refractive index representing the MCh effect. The polarization independence of the MCh effect is attributed to the product of the polarization-dependent effects of the MO effect and OA. In this process, we have not assumed internal coupling between the OA and the MO effect. Our formulation indicates that an MCh effect is realized by combining magnetic and chiral elements. Next, we numerically show that the MCh effect in a metamaterial with broken space and time inversion symmetries well represents the results of our theory.

III. DEMONSTRATION OF THE MCh EFFECT WITHOUT INTERNAL COUPLING

Figure 2 shows an MCh metamaterial composed of chiral and magnetic meta-atoms. The chiral meta-atom consists of two Al nanorods orthogonal to each other, representing the two coupled oscillators. The rods measure 40 × 40 × 100 nm, are spaced 70 nm apart, and are arranged so that the system has C_4 symmetry [17]. The permittivity of Al is modeled by the Drude-Lorentz model [18], in which permittivity has no off-diagonal component. To include nonreciprocity, we introduce a magnetic nanoparticle as a magnetic meta-atom at the center of the chiral structure and assume that an external magnetic field is applied along the $+z$ direction. The radius of the particle is 100 nm. This meta-atom modulates the electromagnetic response of the chiral meta-atoms, giving rise to the MCh effects. The diagonal and off-diagonal components

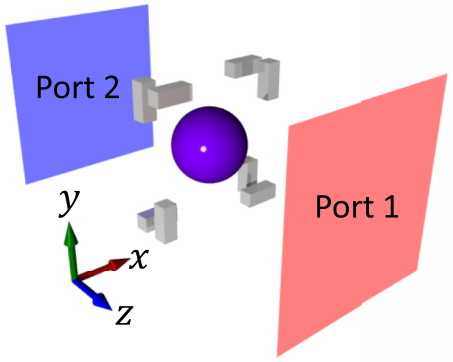

FIG. 2. Schematic of MCh metamaterial. A magnetic nanoparticle is located at the center of the MCh metamaterial. The chiral meta-atom consists of a pair of Al nanorods configured so that the metamaterial has C_4 symmetry.

of permittivity of the magnetic meta-atom are 2.6^2 and $0.2i$, respectively. The eigenstates of the magnetic and chiral meta-atoms are circular polarization. This means that the eigenmodes of the combined structure (the MCh metamaterial) are also circular polarization. The period and total thickness of the MCh metamaterial are 500 nm in the x and y directions and 110 nm, respectively. This thickness is shorter than the wavelength in the deep ultraviolet region, indicating that the MCh metamaterial can be regarded as a subwavelength structure in the wavelength region longer than 220 nm. We introduced x-polarized light into the metamaterial from ports 1 and 2. Both ports are defined to calculate the x component of the fields and are terminated by perfectly matched layers. Under these conditions, we calculated transmission coefficients from the ports as S_{21} and S_{12} by a finite-element method in COMSOL Multiphyiscs software.

Figure 3 shows the phase and amplitude difference spectra of S_{21} and S_{12}. The left and right y axes show the phase and amplitude differences. Owing to the nonreciprocity of the MCh metamaterial, their significant differences are evident. In particular, the differences show clear resonance features and become prominent around 240.4, 256, and 290 nm. The spectra have a dispersive feature around 240.4 nm and, less clearly, around 265 and 290 nm. Hence, we focus on the resonance around 240.4 nm.

To clarify the eigenmode responsible for this strong nonreciprocity, we calculated the near-field distribution patterns of the electromagnetic fields. Figure 4 shows the electric-field

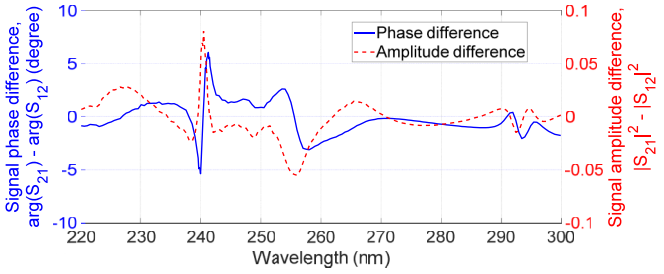

FIG. 3. Signal phase (left) and amplitude (right) difference spectra of the MCh metamaterial.

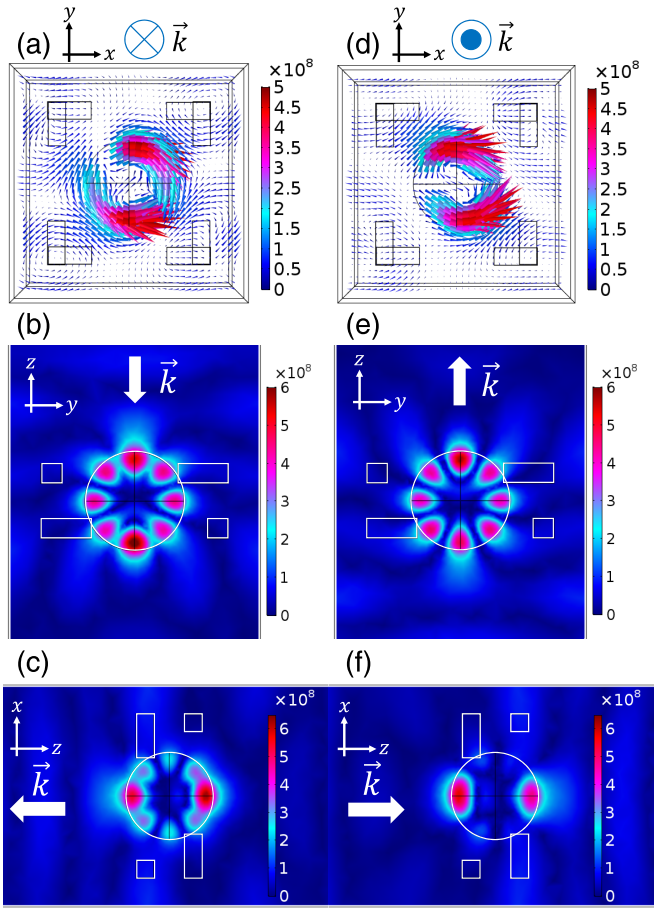

FIG. 4. Electric-field distributions at 240.4 nm when excited from (a)–(c) port 1 and (d)–(f) port 2. Colors indicate electric-field intensities; arrows indicate vectors. The unit of the electric-field intensity is V/m.

distributions at the maximum of the amplitude difference. In Figs. 4(a) and 4(d), the electric-field vectors exhibit dipolelike patterns, indicating that this resonance is related to Mie resonance. The direction of the electric dipole is tilted about 45° in Fig. 4(a) but is nearly horizontal in (d). In addition to the field distributions in the magnetic sphere, those near the chiral meta-atoms are different. The presence of vortexlike features in the upper right and lower left chiral meta-atoms in Fig. 4(a) and their absence in Fig. 4(d) indicates that strong chiral resonance is present only in Fig. 4(a). In Figs. 4(b) and 4(e), the electric-field intensity distributions in the y-z plane have a whispering gallery mode (WGM) characteristic. As shown in Fig. 4, there are two resonances in the metamaterial around 240.4 nm. On the other hand, the distribution patterns in Figs. 4(c) and 4(f) are different from the others: the WGM is excited also in the z-x plane in Fig. 4(c) but not in Fig. 4(f). This result indicates that the resonance condition for WGM in the z-x plane is not satisfied when excited from port 2 owing to the nonreciprocity, resulting in the large transmittance difference. This sensitivity of the resonance condition in a nonreciprocal system has been reported before [10,11].

We calculated the eigenmodes involving the nonreciprocity. To compare the results with our theoretical results,

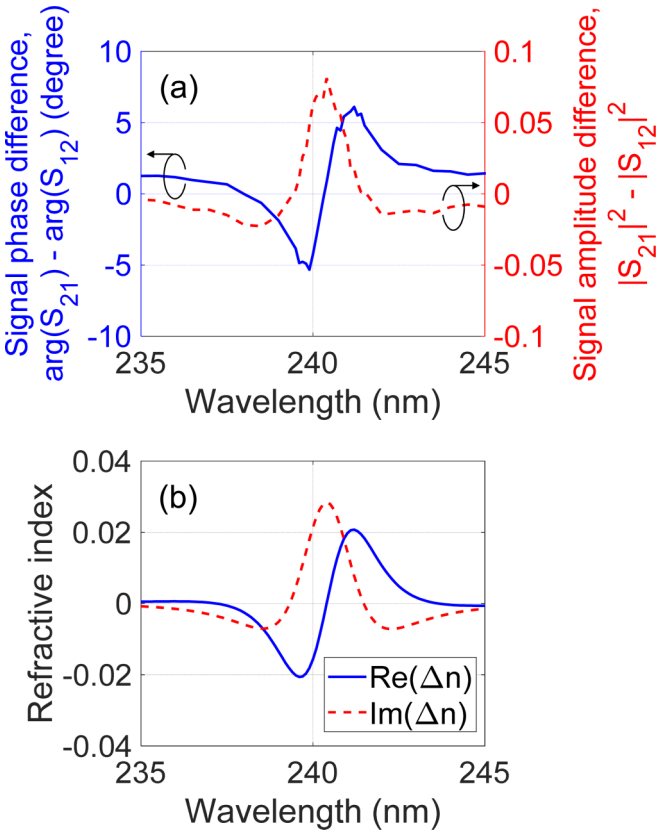

FIG. 5. (a) Phase (left) and amplitude (right) difference spectra of the MCh metamaterial. (b) Real (solid line) and imaginary (dashed line) parts of Δn given by Eq. (17) as a function of wavelength.

we considered the phase and amplitude difference spectra, $S_{21} - S_{12}$. The phase difference corresponds to the difference of the real part of the refractive index, whereas the amplitude difference corresponds to that of the imaginary part. From Eq. (16), the refractive index independent of the polarization state is $\sqrt{\varepsilon} - \xi \mathrm{sgn}(k) g/(\varepsilon - 1)$. The directional birefringence independent of the polarization state is calculated to be

$$\Delta n = \frac{n_k - n_{-k}}{2} = -\xi \frac{g}{\varepsilon - 1}. \tag{17}$$

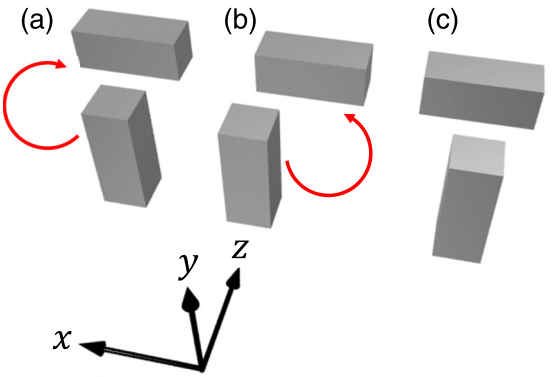

FIG. 6. Schematic of (a) right-handed, (b) left-handed, and (c) achiral meta-atoms. Red arrows in (a) and (b) indicate the twist direction to the $+z$ direction.

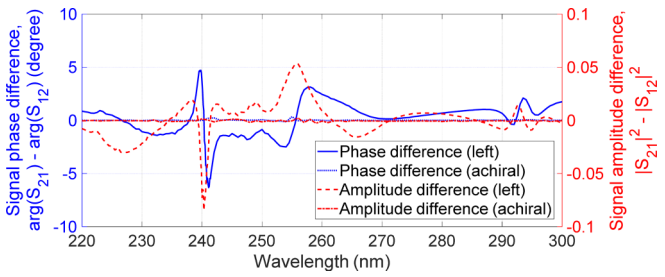

FIG. 7. Signal phase (left) and amplitude (right) difference spectra of the MCh metamaterials with left-handed and achiral meta-atoms.

Figure 5(a) shows an enlarged version of Fig. 3 around 240.4 nm, and Fig. 5(b) shows the real and imaginary parts of Δn. We set the resonance wavelength as 240.4 nm and the damping constant as 0.08 eV. As evident from the comparison between these two figures, there is a clear correspondence between the phase difference and the real part of Δn. The amplitude difference also corresponds to the imaginary part of Δn. The spectral features agree well with the numerical results, indicating that the MCh effect without internal coupling is realized in the MCh metamaterial. To confirm that the nonreciprocity signal is due to the product of ξ and g, we investigated chirality dependence: we switched the chirality of the chiral meta-atom from right [Fig. 6(a)] to left [Fig. 6(b)] or achiral [Fig. 6(c)] and calculated the nonreciprocal response.

Figure 7 shows the signal difference spectra for the MCh metamaterials with left and achiral meta-atoms. The polarity of the nonreciprocity signal of the left-handed structure is reversed from that of the right-handed one of the same magnitude. Moreover, there is no nonreciprocity when the metamaterial has no chirality. These results indicate that the nonreciprocity signal is an odd function with respect to chirality. In addition, we confirmed that the polarity is reversed when the direction of the external dc magnetic field is reversed (not shown). In the absence of the external field, the nonreciprocity disappears (not shown). All these calculations indicate that the nonreciprocity signal is an odd function with respect to ξ and g and originates from the MCh effects represented by the product of ξ and g. The MCh effect in this study is very large and an order of magnitude greater than reported in previous studies in the optical region. Moreover, the gigantic nonreciprocity is realized in the absence of the internal coupling between magnetism and chirality at room temperature. This feature extends the range of application of MCh effects and is thus preferable for practical applications. Thus, a gigantic MCh effect in a metamaterial is key to realizing novel functional devices such as one-way mirrors in the optical region.

IV. CONCLUSION

In summary, we have formulated an MCh effect based on the Born-Kuhn model subject to an external static magnetic field. The MCh effect is represented by the product of the off-diagonal component of permittivity and the chiral parameter, indicating that an MCh effect is induced even in the absence of internal coupling between magnetism and chirality. We have numerically shown that such an MCh effect is realized in a metamaterial composed of magnetic and chiral meta-atoms. Moreover, the MCh effect is gigantically enhanced by the resonance of the metamaterial. This study paves the way to realizing giant MCh effects in the optical region.

ACKNOWLEDGMENTS

The authors acknowledge Kei Sawada, Satoshi Tomita, and Tetsuya Ueda for fruitful discussion. This study was partially supported by the ASTEP program (Grant No. AS2715025R) from the Japan Science and Technology Agency (JST).

[1] G. L. J. A. Rikken and E. Raupach, Nature **390**, 493 (1997).
[2] G. L. J. A. Rikken and E. Raupach, Phys. Rev. E **58**, 5081 (1998).
[3] G. L. J. A. Rikken, C. Strohm, and P. Wyder, Phys. Rev. Lett. **89**, 133005 (2002).
[4] C. Koerdt, G. Düchs, and G. L. J. A. Rikken, Phys. Rev. Lett. **91**, 073902 (2003).
[5] K. Sawada and N. Nagaosa, Phys. Rev. Lett. **95**, 237402 (2005).
[6] H. Kurosawa and K. Sawada, Phys. Rev. A **95**, 063846 (2017).
[7] S. Kibayashi, Y. Takahashi, S. Seki, and Y. Tokura, Nat. Commun. **5**, 4583 (2014).
[8] Y. Nii, R. Sasaki, Y. Iguchi, and Y. Onose, J. Phys. Soc. Jpn. **86**, 024707 (2017).
[9] S. Tomita, K. Sawada, A. Porokhnyuk, and T. Ueda, Phys. Rev. Lett. **113**, 235501 (2014).
[10] S. Tomita, H. Kurosawa, K. Sawada, and T. Ueda, Phys. Rev. B **95**, 085402 (2017).
[11] S. Tomita, H. Kurosawa, T. Ueda, and K. Sawada, J. Phys. D: Appl. Phys. **51**, 083001 (2018).
[12] S. Eslami, J. G. Gibbs, Y. Rechkemmer, J. van Slageren, M. Alarcón-Correa, T.-C. Lee, A. G. Mark, G. L. J. A. Rikken, and P. Fischer, ACS Photon. **1**, 1231 (2014).
[13] G. Armelles, A. Cebollada, H. Y. Feng, A. García-Martín, D. Meneses-Rodríguez, J. Zhao, and H. Giessen, ACS Photon. **2**, 1272 (2015).
[14] V. Yannopapas and A. G. Vanakaras, ACS Photon. **2**, 1030 (2015).
[15] T. Garel, Eur. J. Phys. **24**, 507 (2003).
[16] M. Schäferling, *Chiral Nanophotonics* (Springer-Verlag, Berlin, 2016).
[17] X. Yin, M. Schäferling, B. Metzger, and H. Giessen, Nano Lett. **13**, 6238 (2013).
[18] A. D. Rakić, A. B. Djurišić, J. M. Elazar, and M. L. Majewski, Appl. Opt. **37**, 5271 (1998).